# SMALL-STRAIN DAMPING FOR GROUND RESPONSE ANALYSIS AS USED IN NON-ERGODIC HAZARD ANALYSIS – LESSONS FROM CALIFORNIA RECORDINGS

Kioumars Afshari and Jonathan P. Stewart

Department of Civil & Environmental Engineering
University of California, Los Angeles

## Abstract

We compile a California vertical array database of 21 sites. Weak motion transfer functions derived from data are compared to predictions from 1D ground response analyses performed using three damping models – geotechnical models, models for quality factor ($Q$) based on seismological inversion, and models derived from the site-specific site diminutive parameter ($\kappa_0$). When compared to prior results for KiK-net sites in Japan, the California sites have, on average, improved match of empirical and theoretical transfer function shapes and more event-to-event consistency. Using $\kappa_0$-informed damping results in a slightly better fit between predicted and observed transfer functions than alternative damping models.

## Introduction

Evaluating the role of local site conditions on ground shaking is an essential part of earthquake ground motion prediction, which can be done using ergodic models or site-specific (non-ergodic) analyses. One-dimensional (1D) simulation of shear waves propagating vertically through shallow soil layers, also known as ground response analysis (GRA), is a common approach for capturing the effects of site response on ground shaking. While site response can include important contributions from the wave propagation mechanics simulated in GRA, site response as a whole is considerably more complex. Processes that can control site response in this context include 1D ground response in combination with additional effects including surface waves, basin effects (including focusing and basin edge-generated surface waves), and topographic effects. Because GRA only simulates a portion of the physics controlling site response, there should be no surprise that it is not always effective at accurately predicting site effects.

Validation and testing of 1D GRA is possible by studying recordings from vertical array sites. They allow for the observation of ground motions from the same source both at the surface and the depth at which the downhole sensor is installed. Therefore, a vertical array directly reveals the effects of site response between surface and downhole instruments. In addition, well characterized vertical array sites, which include a high quality shear wave velocity ($V_S$) profile and possibly a geotechnical log, allows for validating numerical site response models.

Numerous studies of data from vertical arrays at individual sites have found reasonably good fits of data to GRA results (e.g., Borja et al., 1999; Elgamal et al., 2001; Lee et al., 2006; Tsai and Hashash, 2009; Yee et al., 2013). The KiK-net array in Japan (Aoi et al., 2000) provides

a large inventory of vertical arrays that has been extensively used for validation purposes (Thompson et al., 2012; Kaklamanos et al, 2013, 2015; Zalachoris and Rathje, 2015), although the resolution and quality of the seismic velocity and geotechnical site descriptions is arguable sub-optimal. Nonetheless, when viewed as a whole, these KiK-net data challenge the notion that 1D GRA provides a reliable estimate of site response. Were this result found to be widely applicable, it would upend a good deal of current practice that relies on GRA to estimate first-order site response.

Our objective in this study was to evaluate ground response analysis as a method of predicting non-ergodic (site-specific) site response. We utilize the growing body of vertical array data from California which we compiled into a database described in Chapter 2 of Afshari and Stewart (2017). We use the data to evaluate surface-downhole transfer functions, and we study the goodness of fit between empirical transfer functions (ETF) from observations and theoretical transfer functions (TTF) from 1D GRA. In 1D GRA, we use three different approaches for estimating soil damping as discussed next. This paper extends upon the preliminary results presented in Afshari and Stewart (2015) using more sites and an additional damping model informed by site-specific observations regarding high-frequency spectral decay using the so-called diminutive parameter ($\kappa_0$).

## Ground Response Analyses Procedures

There are many options for performing 1D GRA. Different procedures for GRA can be used depending on the level of nonlinearity that is expected in the profile. The principal alternatives for GRA are linear (more specifically, visco-elastic), Equivalent-Linear (EL), and Nonlinear (NL) methods. Linear methods require only a shear wave velocity profile, unit weights, and a soil damping profile. Additional soil properties required for EL are relationships for modulus reduction and damping vs. shear strain. The NL procedures require these same inputs, but will often incorporate shear strength and other parameters related to viscous damping and rules for unload-reload relationships.

We model the soil as linearly visco-elastic because almost all of the recordings compiled in our database are not strong enough to cause soil nonlinearity. Therefore, we only perform linear analysis to validate GRA under small levels of ground shaking. We have chosen to use the linear option in the Frequency Domain Analysis module in DEEPSOIL (Hashash et al., 2016) for linear analysis. We applied parameter selection protocols for GRA as given by Stewart at al. (2014). An exception is small strain damping ($D_{min}$), the selection of which is discussed below.

## Alternative Damping Models

Small-strain damping is required in GRA, including those employing linear soil properties. Even under elastic conditions, damping occurs because of the intrinsic damping within soil elements and scattering of waves off of subsurface irregularities (e.g., Rodriguez-Castellanos et al. 2006).

We consider two classes of models for small strain damping in soils, both of which are frequency-independent (hysteretic). The first class of models are collectively referred to as geotechnical models, because they are derived from advanced cyclic testing performed in

geotechnical labs. These models account for intrinsic damping. The second are $V_S$-based models originally developed from calibration of stochastic ground motion simulations in central and eastern North America. To the extent that the calibration is accurate for a given application, these models incorporate the effects of both intrinsic material damping and scattering.

## Material Damping Models

Various geotechnical models relate small-strain damping as measured from geotechnical laboratory cyclic testing, denoted $D_{min}^{L}$, to various predictor variables related to soil type and confining pressure. We estimate laboratory-based $D_{min}^{L}$ using Darendeli (2001) relations for clays and silts, and Menq (2003) relations for granular soils. The input parameters for the $D_{min}^{L}$ models are plasticity index (*PI*), overconsolidation ratio (*OCR*), and effective stress for Darendeli (2001), and mean grain size ($D_{50}$), coefficient of uniformity ($C_u$), and effective stress for Menq (2003). The $D_{min}^{L}$ relations can only be used when geotechnical log and/or description of soil conditions are available for the site.

## Models for Combined Material Damping and Wave Scattering Effects

We begin with a brief description of the square-root impedance (SRI) method for predicting site effects (Joyner et al. 1981; Boore 2013). While this method is not directly used for comparison to data in this study, the approach is nonetheless important for the present discussion because it provides the context in which site diminutive parameter $\kappa_0$ is used. The SRI method uses the following equation for evaluating amplification of Fourier Amplitude Spectra for a vertical ray path:

$$A_0(f) = \left( \frac{\rho_R V_R}{\overline{\rho}\,\overline{V}} \right)^{0.5} \tag{1}$$

where $A_0$ is the amplification, $\rho_R$ and $V_R$ are density and shear wave velocity at the reference (downhole condition), and $\overline{\rho}$ and $\overline{V}$ are average density and shear wave velocity for a depth interval corresponding to the top quarter wavelength of the profile. While this method is simple and efficient, it cannot capture the effects of resonance and nonlinearity. Moreover, in the form represented by Eq. (1), it does not include the effects of damping, which is evident by the amplification value at high frequencies approaching a plateau. This plateau feature is unrealistic because actual amplification functions slope downward with frequency at high frequencies beyond the primary modal peaks in the spectrum. Although the shape shown in Figure 1 is strictly applicable to site amplification, similar features are observed in simulated Fourier amplitude spectra using stochastic methods (e.g., Boore, 2003).

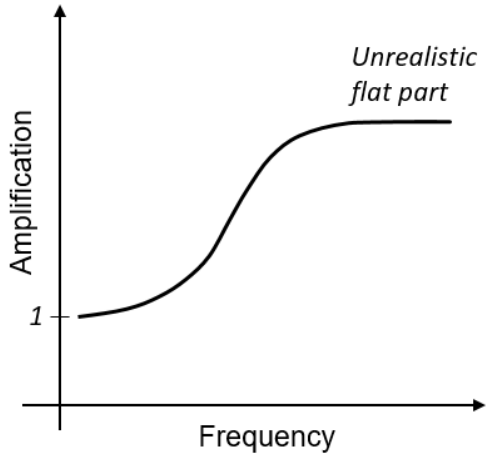


**Figure 1.** Unrealistic plateau of amplification at high frequencies when using quarter wave length theory without application of diminutive parameter $\kappa$.

In order to overcome the problem of unrealistic Fourier amplitude spectral shapes at high frequencies, a spectral decay, or diminutive, parameter ($\kappa$) is introduced.

$$X(f) = X_0(f) \times \exp(-\pi\kappa f) \tag{2}$$

where $X$ indicates Fourier amplitude. The effect on spectral shape of applying this parameter is shown in Figure 2. The value of $\kappa$ applicable to a particular ground motion recording can be partitioned into two components, namely a zero distance $\kappa$ or site $\kappa$ ($\kappa_0$), and the attenuation with distance ($\kappa_R R$) (adapted from Anderson, 1991):

$$\kappa = \kappa_0 + \kappa_R R \tag{0}$$

where $R$ is the source-site distance, and $\kappa_R$ is the rate with which the decay parameter ($\kappa$) increases with distance, capturing the effects of anelastic attenuation.

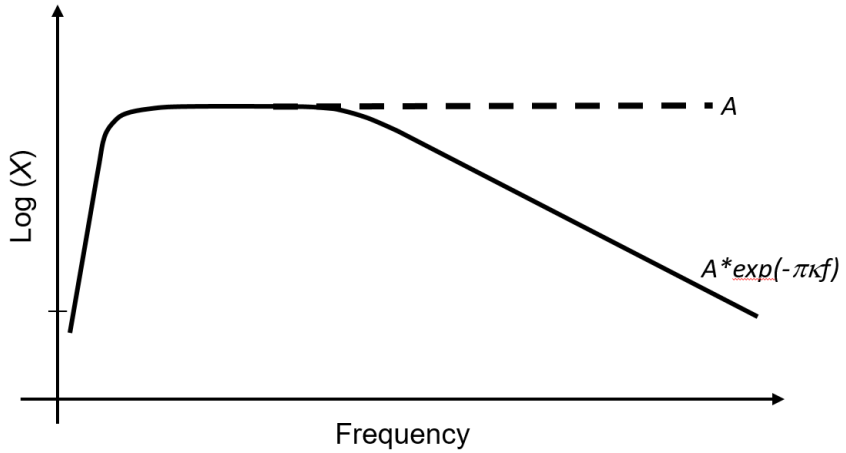


**Figure 2.** Modifying simulated ground motions at high frequencies by introducing $\kappa$.

The contribution of site damping to high frequency attenuation is captured by the $\kappa_0$ diminutive parameter (Eq. 3). The $\kappa_0$ parameter represents the cumulative effect of damping through the soil column, which is commonly represented by (Hough and Anderson 1988; Chapman et al. 2003; Campbell 2009):

$$\kappa_0 = \int_0^z \frac{dz}{Q_{ef}(z) V_S(z)} \tag{4}$$

where $z$ is the soil column depth and $Q_{ef}$ is the depth-dependent effective material quality factor, representing both the effects of frequency-dependent wave scattering and frequency-independent soil damping. Quantity $Q_{ef}$ can be readily converted to an effective soil damping as follows (Campbell, 2009):

$$D_{eff}(\%) = \frac{100}{2Q_{\text{ef}}} \tag{5}$$

In order to facilitate ground motion prediction in central and eastern U.S., several investigators have developed models for either depth-dependent $Q_{ef}$ or $\kappa_0$ in particular regions (e.g., Boore and Joyner 1991, Gomberg et al. 2003, Cramer et al. 2004). Campbell (2009) reviewed many of these studies and proposed a suite of models relating $Q_{ef}$ to $V_S$, one of which is given by:

$$Q_{ef} = 7.17 + 0.0276 V_S \tag{6}$$

where $V_S$ is in m/s. Eq. (6) is one of four models proposed by Campbell (2009) and has seen application in a number of subsequent studies (Hashash et al., 2014; E. Rathje, personal communication) (more so than the other three models). We choose to use this model over an older model by Olsen et al. (2003) which is intended for long periods (>2 sec). An advantage of this approach for modeling $D_{eff}$ is that it is only based on $V_S$ as an input parameter, and therefore it does not require a geotechnical log. We apply this approach for all 21 sites used in this study.

The third damping model considered in this study takes the site component of $\kappa$ (i.e, $\kappa_0$) from ground motion recordings to adjust values of small-strain damping derived from geotechnical models to represent site-specific effects. Whether such adjustments are effective for ground motion prediction is investigated in the next section.

The expression for $\kappa_0$ given in Eq. (4) strictly applies when the full crustal profile is considered in the depth integral. A more practical alternative is to evaluate the site diminutive parameter for reference rock, $\kappa_{0,ref}$, and then modify it for damping through the soil column as (Campbell, 2009):

$$\kappa_0 = \kappa_{0,ref} + \int_0^z \frac{dz}{Q_{ef}(z) V_S} \tag{7}$$

The integral in this case represents the contribution from the geologic column above the reference rock. Note that $\kappa_{0,ref}$ as used in simulations may not match the site condition at the downhole sensor. However, for the present application, we take $\kappa_{0,ref}$ as applying for the

downhole geologic condition. Adopting this definition and using Eq. (5) to convert $Q_{ef}$ to $D_{min}$, we re-write Eq. (7) as:

$$\kappa_0 = \kappa_{0,ref} + \int_0^z \frac{2D_{eff}(z)}{100} V_S^{-1}(z)dz \quad (8)$$

The vertical array data can be used to estimate the integral in Eq. (8), which in turn can be used to adjust model-based $D_{min}$ to reflect site-specific conditions. The methodology of estimating $\kappa$-informed damping is described in Section 3.2.3 of Afshari and Stewart (2017).

## Inferences of Site Response from Transfer Functions and Implications for the Effectiveness of Ground Response Analysis

Empirical transfer functions (ETFs) representing site response between the downhole and surface accelerometers are computed from ratios of Fourier amplitudes as follows:

$$H(f) = \frac{Z(f, x_1)}{X(f, x_2)} \quad (9)$$

where $H(f)$ is the ETF, $Z(f,x_1)$ is the surface FAS and $X(f,x_2)$ is the downhole FAS. ETFs are only considered over the usable frequency range based on record processing. The ETF is taken as the geometric-mean of ETFs for the two horizontal components of the recordings (at their as-recorded azimuths) for each site. The results shown subsequently are smoothed through the use of a logarithmic window function proposed by Konno and Ohmachi (1998) with the coefficient for bandwidth frequency ($b$) equal to 20.

Theoretical transfer functions (TTF) are a direct outcome of linear analysis. In other words, the calculation of TTFs does not require analysis of ground motions and their Fourier amplitudes as in Eq. (9). When time-domain procedures are used, the ground motions must be calculated, their FAS computed, and then TTF can be taken using Eq. (9).

Before proceeding further, it should be pointed out that the ETF (and TTF) represents the surface/downhole ratio in which the surface motion is outcropping and the downhole motion is 'within'. The 'within' term indicates that the motion includes the effects of down-going waves that have reflected from the ground surface, whereas outcropping motions are twice the amplitude of the incident wave due to full reflection at a free-surface.

### Transfer Function Comparisons from KiK-Net Array in Japan

Thompson et al. (2012) studied 100 KiK-Net sites in Japan in order to assess the variability in site amplification and the performance of linear 1D GRA. These sites have recorded a large number of surface and downhole recordings. For GRA, they used the program NRATTLE, which is a part of the ground motion simulation program SMSIM (Boore, 2005). NRATTLE performs linear GRA using Thomson–Haskell matrix method (Thomson, 1950; Haskell, 1953). The input parameters for NRATTLE include shear wave velocity ($V_S$), soil density, and the intrinsic attenuation of shear-waves ($Q_S^{-1}$) which represents damping. Soil density was estimated from P-wave velocity using the procedures suggested by Boore (2008), and $Q_S^{-1}$was estimated using a grid-search algorithm to optimize the fit to $H(f)$. Note that by

optimizing damping in this manner, Thompson et al. (2012) do not assess the performance of alternative damping models. Moreover, this optimization would not be possible to perform in a forward sense when vertical array recordings from a site are not available.

Thompson et al. (2012) computed ETFs with Eq. (9) using available data meeting certain selection requirements. In order to minimize the potential for nonlinear effects, only records having a ground surface PGA < 0.1 g were selected. In total, 3714 records from 1573 earthquakes were considered for the 100 KiK-net sites. Goodness-of-fit was quantified using Pearson's sample correlation coefficient ($r$) as a measure of how well the model predictions and the data are correlated. Parameter $r$ quantifies how well the transfer functions align, including the locations and shapes of peaks. Parameter $r$ is insensitive to relative overall levels of amplification. Thompson et al. (2012) calculated the Pearson's sample correlation coefficient for $i^{th}$ earthquake and $j^{th}$ analysis (based on damping estimation approach) as follows for a given site:

$$r_{ij} = \frac{\sum\left(\mathrm{ETF}_i(f) - \overline{\mathrm{ETF}_i}\right)\left(\mathrm{TTF}_j(f) - \overline{\mathrm{TTF}_j}\right)}{\sqrt{\sum\left(\mathrm{ETF}_i(f) - \overline{\mathrm{ETF}_i}\right)^2}\sqrt{\sum\left(\mathrm{TTF}_j(f) - \overline{\mathrm{TTF}_j}\right)^2}} \tag{10}$$

The summations in Eq. (10) are taken over a frequency range with a lower bound $f_{min}$ corresponding to the first peak in the TTF and an upper bound $f_{max}$ that is the minimum of the frequency of the fourth peak of the TTF or 20 Hz. The summation is performed over all frequency points between $f_{min}$ and $f_{max}$, which are equally spaced in logarithmic units. The mean value of $r$ across all events ($r_j$) for a given site is denoted $\bar{r}$. A value of $\bar{r} = 0.6$ was taken by Thompson et al. as the threshold for good fit.

Results for the 100 considered KiK-Net sites show that only 18% have a good fit between ETFs and TTFs, indicating 1D GRA fails to provide an accurate estimation of site response for a large majority of KiK-net sites.

A second metric considered by Thompson et al. (2012) concerns the inter-event variability of transfer function ordinates, which they computed as a median value of the standard deviations computed across the frequencies within the range to compute $r$. Large values of this standard deviation indicate large event-to-event differences in observed site amplification, suggesting potential complexities from 3D geologic structure. The results for full list of 100 sites and a comparison to California data is presented in the next section.

## Transfer Function Comparisons for California Vertical Array Data

Using the data set described in Chapter 2 of Afshari and Stewart (2017), we compute ETF ordinates for each of 21 selected California vertical array sites. In this sense our approach is similar to that of Thompson et al. (2012) – we 'cast the net widely' to study site response performance over a wide range of conditions. Unlike several studies conducted since Thompson et al. (2012), we do not screen sites to identify those for which the ETF matches the shape of a TTF; instead we seek to understand how frequently such a match is achieved in relatively weak motion data from California vertical array sites.

We exclude recordings with strong ground shaking (*PGA* at surface instrument > 0.1 g) so as to minimize nonlinear effects. Figure 3 shows histograms of *PGA* and *PGV* for the downhole instrument records used in the present work.

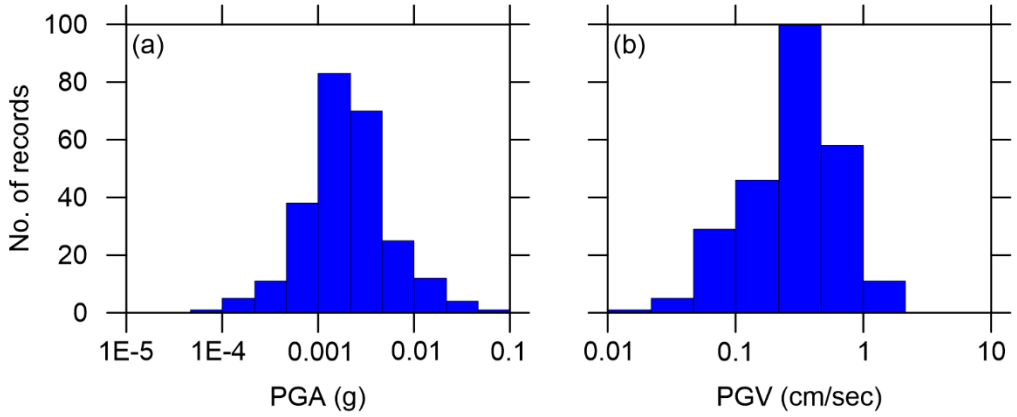


**Figure 3.** Histograms of PGA (a) and PGV (b) for downhole recordings used in this study

We assume a log-normal distribution for ETF ordinates and compute for each site the median ($\mu_{\ln}$) (equivalent to the exponent of the natural log mean) and the natural log standard deviation of ETF ($\sigma_{\ln}$) at each frequency using all available record pairs.

Theoretical transfer functions (TTFs) are computed by linear visco-elastic 1D GRA in DEEPSOIL (Hashash et al., 2016). As the downhole sensor is recording both up-going and down-going waves, we take the boundary condition at the base of the model as rigid (Kwok et al., 2007). The visco-elastic analysis in DEEPSOIL is performed in the frequency domain, and the transfer function predicted by the model is independent of the input motion. Similar to ETFs, the TTFs are smoothed by Konno and Ohmachi (1998) function with $b$=20. We utilize alternate approaches for estimating small-strain soil damping as described previously to provide insight and guidance on best practices for selection of effective small-strain damping ($D_{eff}$). Note that this aspect of our analysis departs from the prior work of Thompson et al. (2012), who back-calculated damping to optimize the ETF-TTF fit.

Figure 4 shows two examples of model-data transfer function comparisons. The match (or lack thereof) of the positions of the first several peaks in ETFs and TTFs are a good indicator of consistency between the transfer functions. In the example of El Centro-Meloland site, the simulations are not able to capture the position of any of the visible five peaks seen in the ETF. This is an indication that 1D GRA is unable to simulate the site response between surface and downhole regardless of the damping model. On the contrary, for the Treasure Island site, the position of all six peaks in the ETF are captured by GRA, which is an indication that the 1D assumption implicit to GRA is valid for this site.

We also consider the quantitative assessment of goodness of fit provided by the Pearson's sample correlation coefficient $r$ (Eq. 10). We use the mean value over all recordings at a given site, $\bar{r}$, which is shown in Figure 5. Generally, sites with qualitatively good fit between ETF and TTF have values of $\bar{r} > 0.6$ (e.g., Treasure Island site in Figure 4) and sites with poor fit have

$\bar{r} < 0$ (e.g., El Centro-Meloland site). Transfer function comparisons for the other 19 vertical array sites are given in Chapter 4 of Afshari and Stewart (2017).

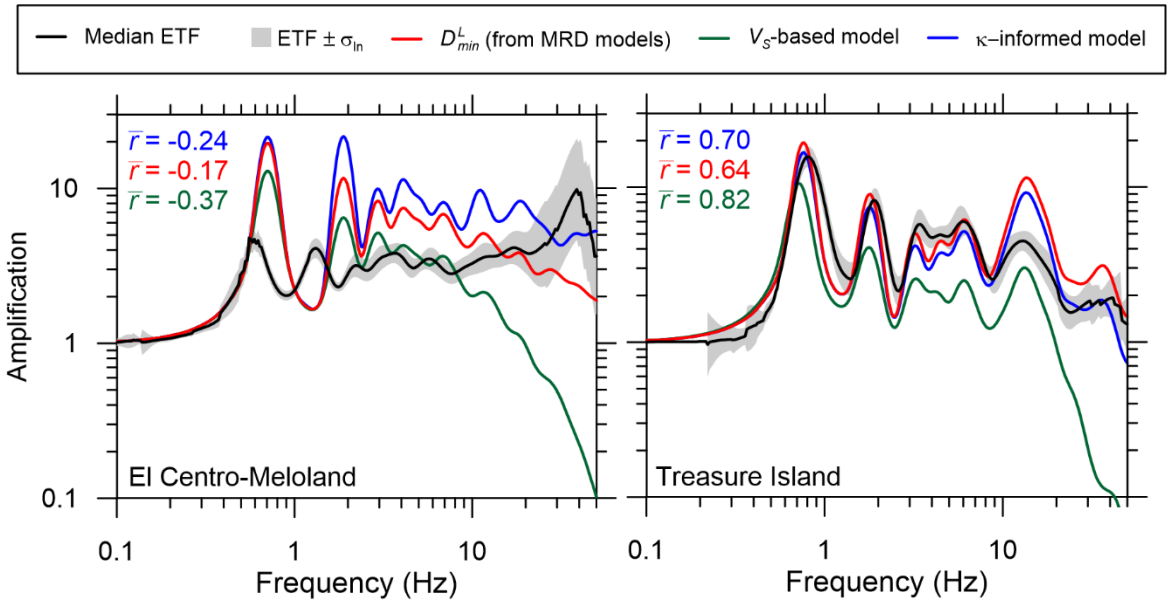


**Figure 4.** Comparison of ETF and TTFs for El Centro-Meloland and Treasure Island. Values of $\bar{r}$ for each damping model are shown in different colors (red: $D^L_{min}$, green: $V_S$-based, blue: $\kappa$-informed).

Figure 5 shows histograms of $\bar{r}$ from the California vertical array sites using the three damping models (geotechnical, $V_S$-based, $\kappa$-informed). Also shown for comparison is the distribution from Thompson et al. (2012) for KiK-net sites, although the optimization of damping performed in that study makes the comparison somewhat 'apples-to-oranges', with Japan sites expected to have higher $\bar{r}$ than they would have had without optimization. We see that California sites have higher values of $\bar{r}$ in aggregate, with a higher population median and lower standard deviation. There is also a higher percentage of sites with strong correlation ( $\bar{r} >$ 0.6) in comparison to their counterparts for the KiK-net arrays in Japan for all damping models. This suggests that the ability of GRAs to match observation is better for the California vertical arrays than for KiK-net sites. Furthermore, the comparison of $\bar{r}$ histograms for California sites suggests a slight increase in $\bar{r}$ when using the $\kappa$-informed model indicating a slightly better performance of the $\kappa$-informed damping model in capturing the shape of site response transfer functions.

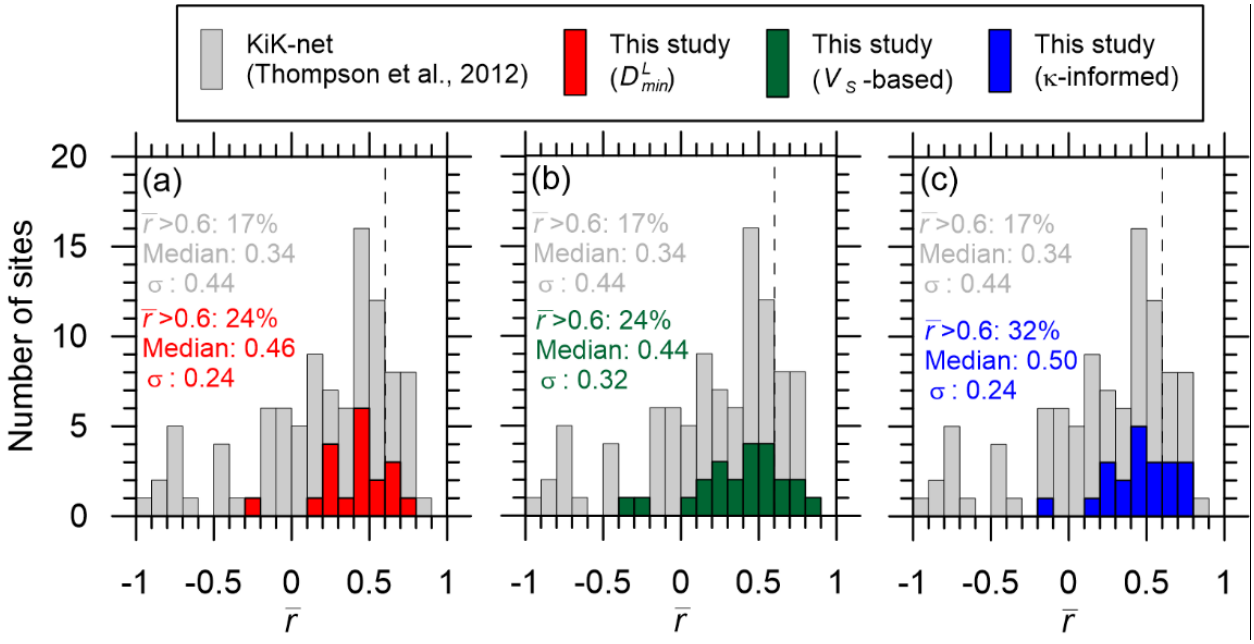


**Figure 5.** Histograms of $\bar{r}$ for California and KiK-net sites as well as their medians and standard deviations. Values and summary statistics of $\bar{r}$ for each damping model are shown in different colors for California sites (red: $D^L_{min}$, green: $V_S$-based, blue: $\kappa$-informed model).

As described earlier, Thompson et al. (2012) introduced a metric of ETF variability that is useful to consider in combination with $\bar{r}$ because it quantifies event-to-event variability in observed site response across a particular vertical array. This metric is computed by first taking the natural log standard deviation of ETF ordinates for each of the frequencies considered in the analysis of $\bar{r}$ (i.e., between the lower and upper bound frequencies $f_{\text{min}}$ and $f_{\text{max}}$). Then the median across those standard deviations is taken, which is denoted $\sigma^M_{ln}$. Figure 6 shows the distribution of $\sigma^M_{ln}$ for the California vertical array sites, with the values reported by Thompson et al. (2012) for the KiK-net sites also shown for comparison (the method of computation is the same in both cases). The inter-event dispersion is notably smaller for the California sites, with only two (10%) exceeding the value of 0.35 considered as 'high dispersion' by Thompson et al. (2012).

Sites having comparable transfer function shapes and low dispersion have been useful for GRA validations performed in several studies (e.g., Kaklamanos et al. 2015, Zalachoris and Rathje, 2015). To facilitate similar work using California data, Table 1 lists California vertical array sites with $\bar{r} > 0.6$ and $\sigma^M_{ln} < 0.2$ (considering the most optimal outcomes among the damping models).

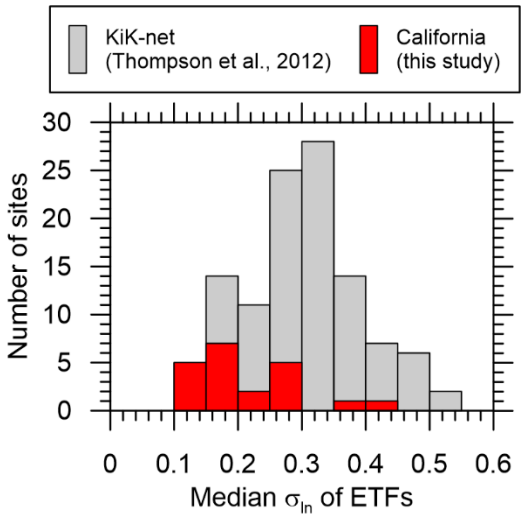


**Figure 6.** Histogram of ETF between-event standard deviation term $\sigma_{ln}^{M}$ for California and KiK-net vertical array sites.

**Table 1.** California vertical array sites with $\bar{r} > 0.6$ and $\sigma_{ln}^{M} < 0.2$ (considering the most optimal outcomes among the damping models)

| Site Name | Code # | Optimal $\bar{r}$ | Damping model | $\sigma_{ln}^{M}$ |
|---|---|---|---|---|
| Benicia-Martinez South | 68323 | 0.79 | $V_S$-based | 0.17 |
| Eureka | 89734 | 0.75 | $V_S$-based | 0.20 |
| Treasure Island | 58642 | 0.82 | $V_S$-based | 0.20 |
| Wildlife Liquefaction Array | NA | 0.69 | Geotechnical | 0.15 |

## Summary and Interpretation of Results

California has one of the most useful inventories of vertical arrays world-wide, when viewed from the perspective of site and ground motion data quality and quantity. We have compiled a database that is used to investigate the effectiveness of the 1D assumption inherent to ground response analysis procedures and to evaluate the relative effectiveness of three alternative damping models.

We find a better fit and smaller ETF dispersion for the California sites as compared to what was found previously by Thompson et al. (2012) for 100 KiK-net sites. This may result from the former mostly being located within large sedimentary basins and relatively flat areas, whereas the later are often on firmer ground conditions (often weathered rock or thin soil over rock) with uneven ground conditions. The geologic conditions at the KiK-net sites are such that horizontal layering of sediments is less likely to be an acceptable assumption, with the site response being strongly influenced by 2D and 3D effects associated with irregular stratigraphy and (in some cases) topography. The 2D and 3D effects in site response in KiK-net sites has been studied by De Martin et al. (2013), who suggests the period and amplitude of site response peaks are significantly sensitive to 2D and 3D effects due to non-horizontal layering. Another possible

factor resulting in a better fit for California sites is the quality of $V_S$ measurements. The vertical arrays in California used in this study have high-resolution suspension logging measurements (with only one exception), while the KiK-net sites are characterized with lower-resolution downhole measurements.

Ground response analyses based on geotechnical models underestimate site attenuation, which has been observed previously and is expected because scattering effects are neglected. The models based on seismological inversion tend to overestimate site attenuation; this conclusion is likely not fully general, but applies to the considered data inventory. Among the three damping models used in this study for GRA, the $\kappa$-informed model is found to slightly better predict the shape of site response transfer functions.

## Acknowledgments

Funding for this study is provided by California Strong Motion Instrumentation Program, California Geological Survey, Agreement Numbers 1014-961 and 1016-985. This support is gratefully acknowledged. We are appreciative of Tadahiro Kishida and Yousef Bozorgnia for providing access to data processing codes and their efforts in developing data resources used in this study. We also thank Hamid Haddadi of CSMIP for providing weak motion records from the Center for Engineering Strong Motion Data FTP folders, Javier Vargas Ortiz, Bahareh Heidarzadeh, and Jamison Steidl for providing geotechnical logs for vertical arrays sites considered in this project, and Eric Thompson and Adrian Rodriguez-Marek for providing valuable insight on their previous studies involving vertical arrays.

## References

Afshari, K. and Stewart, J. P., 2015. Effectiveness of 1D ground response analyses at predicting site response at California vertical array sites, *Proc. SMIP2015 Seminar on Utilization of Strong Motion Data*, California Strong Motion Instrumentation Program, Sacramento, CA.

Afshari, K. and Stewart, J. P., 2017. Implications of California Vertical Array Data for the Analysis of Site Response with 1D Geotechnical Modeling, *A report on research conducted under grant no. 1014-961 from California Strong Motion Instrumentation Program, California Geological Survey.*

Anderson, J. G., 1991. A preliminary descriptive model for the distance dependence of the spectral decay parameter in Southern California, *Bull. Seismol. Soc. Am*. 74, 1969-1993.

Aoi, S. ,Obara, K., Hori, S., Kasahara, K., Okada, Y., 2000. New Japanese uphole–downhole strong-motion observation network: KiK-Net, Seismological Research Letters *Seism. Res. Lett.* 72:239.

Boore, D.M., 2003. Simulation of ground motion using the stochastic method, *Pure and Applied Geophysics*, **160**, 635-675.

Boore, D. M., 2005. SMSIM—Fortran programs for simulating ground motions from earthquakes: Version 2.3—A Revision of OFR 96- 80-A, *Open-File Rpt. 00-509*, U.S. Geological Survey, revised 15 August 2005, 55 pp.

Boore, D.M., 2008. Some thoughts on relating density to velocity <http://quake.wr.usgs.gov/boore/daves_notes/daves_notes_on_relating_density_to_velocity_v1.2.pdf>

Boore, D. M., 2013. The uses and limitations of the square-root-impedance method for computing site amplication. *Bull. Seismol. Soc. Am.* **103**, 2356-2368.

Boore, D. M., and W. B. Joyner, 1991. Estimation of ground motion at deep-soil sites in eastern North America, *Bull. Seismol. Soc. Am.* **81**, 2167–2185.

Borja, R. I., Chao, H.-Y., Montans, F. J., and Lin, C.-H., 1999. Nonlinear ground response at Lotung LSST site, *J. Geotech. Geoenviron. Eng.*, **125**, 187–197.

Campbell, K.W., 2009. Estimates of shear-wave *Q* and $\kappa_0$ for unconsolidated and semiconsolidated sediments in Eastern North America, *Bull. Seismol. Soc. Am*. 99, 2365-2392.

Cramer, C. H., Gomberg, J. S., Schweig, J. S., Waldron, B. A., and Tucker, K., 2004. The Memphis, Shelby Country, Tennessee, seismic hazard maps, *U.S. Geol. Surv.* Open-File Rept. 04-1294.

Darendeli, M. B., 2001. Development of a New Family of Normalized modulus reduction and material damping curves, PhD Thesis, Department of Civil Engineering, University of Texas, Austin, TX.

De Martin, F., Matsushima, S., Kawase, H., 2013, Impact of geometric effects on near- surface Green's functions, *Bull. Seismol. Soc. Am*. **103**, 3289-3304.

Elgamal, A., Lai, T., Yang, Z., He, L., 2001. Dynamic soil properties, seismic downhole arrays and applications in practice, *Proceedings, 4th International Conference on Recent Advances in Geotechnical Earthquake Engineering and Soil Dynamics*, S. Prakash, ed., San Diego, CA.

Gomberg, J., Waldron, B., Schweig, E., Hwang, H., Webbers, A., Van Arsdale, R., Tucker, K., Williams, R., Street, R., Mayne, P., Stephenson, W., Odum, J., Cramer, C., Updike, R., Hutson, S., and Bradley, M., 2003. Lithology and shear-wave velocity in Memphis, Tennessee, *Bull. Seismol. Soc. Am*. **93**, 986–997.

Haskell, N.A., 1953. The dispersion of surface waves on multilayered media. *Bull. Seismol. Soc. Am.*, **72**, 17–34.

Kaklamanos, J., Bradley, B. A., Thompson, E. M., and Baise, L. G., 2013. Critical parameters affecting bias and variability in site-response analyses using KiK-net downhole array data, *Bull. Seismol. Soc. Am.*, **103**, 1733–1749.

Kaklamanos, J., Baise, L. G., Thompson, E. M., and Dorfmann, L., 2014. Comparison of 1D linear, equivalent-linear, and nonlinear site response models at six KiK-net validation sites, *Soil Dyn. Eqk. Eng.*, **69**, 435–460.

Kaklamanos, J., Baise, L. G., Thompson, E. M., Dorfmann, L., 2015. Comparison of 1D linear, equivalent-linear, and nonlinear site response models at six KiK-net validation sites, *Soil Dyn. Earthq. Eng.* 69, 207-215.

Konno, K., and Ohmachi, T. (1998). Ground-Motion Characteristics Estimated from Spectral Ratio between Horizontal and Vertical Components of Microtremor, *Bull. Seismol. Soc. Am.*, **88**, 228–241.

Kwok, A.O., Stewart, J.P., Hashash, Y.M.A., Matasovic, N., Pyke, R., Wang, Z., and Yang, Z. (2007). Use of exact solutions of wave propagation problems to guide implementation of nonlinear seismic ground response analysis procedures, *J. Geotech. & Geoenv. Engrg.*, ASCE, 133 (11), 1385-1398.

Lee, C.-P., Tsai, Y.-B., and Wen, K. L., 2006. Analysis of nonlinear site response using the LSST downhole accelerometer array data, *Soil Dyn. Eqk. Eng.*, **26**, 435–460.

Menq, F. Y., 2003. Dynamic Properties of Sandy and Gravelly Soils, PhD Thesis, Department of Civil Engineering, University of Texas, Austin, TX.

Olsen, K., Day, S., Bradley, C., 2003. Estimation of Q for long-period (> 2 sec) waves in the Los Angeles basin. *Bull. Seismol. Soc. Am.* **93**, 627–638.

Rodriguez-Castellanos, A, FJ Sánchez-Sesma, F Luzon, R Martin, 2006. Multiple scattering of elastic waves by subsurface fractures and cavities, *Bull. Seismol. Soc. Am.* **96**, 1359-1374

Stewart, J.P., Afshari, K., and Hashash, Y. M. A., 2014. Guidelines for performing hazard-consistent one-dimensional ground response analysis for ground motion prediction, *PEER Report No. 2014/16*, Pacific Earthquake Engineering Research Center, UC Berkeley, CA.

Thompson, E. M., Baise, L. G., Tanaka, Y., and Kayen, R. E., 2012. A taxonomy of site response complexity, *Soil Dyn. Earthq. Eng.*, **41**, 32–43.

Thomson, W. T., 1950. Transmission of elastic waves through a stratified solid, Journal of Applied Physics, **21**, 89–93.

Tsai, C. C. and Hashash, Y. M. A., 2009. Learning of dynamic soil behavior from downhole arrays, *J. Geotech. Geoenv. Eng.*, **135**, 745–757.

Yee, E., Stewart, J. P., and Tokimatsu, K., 2013. Elastic and large-strain nonlinear seismic site response from analysis of vertical array recordings, *J. Geotech. Geoenv. Eng.*, **139**, 1789–1801.

Zalachoris, G., and Rathje E. M., 2015. Evaluation of one-dimensional site response techniques using borehole arrays, *J. Geotech. Geoenviron. Eng.*, 10.1061/(ASCE)GT.1943-5606.0001366, 04015053.